# Flow Pattern and Oil Holdup Prediction in Vertical Oil–Water Two–Phase Flow Using Pressure Fluctuation Signal

***Azizi, Sadra; Karimi, Hajir*[+]; Darvishi, Parviz***

*Department of Chemical Engineering, Yasouj University, P.O. Box 75914-353 Yasouj, I.R. IRAN*

**ABSTRACT:** *In this work, feasibility of flow pattern and oil holdup prediction for vertical upward oil–water two–phase flow using pressure fluctuation signals was experimentally investigated. Water and diesel fuel were selected as immiscible liquids. Oil holdup was measured by Quick Closing Valve (QCV) technique, and five flow patterns were identified using high-speed photography through a transparent test section with Inner Diameter (ID) of 0.0254 m. The observed flow patterns were Dispersed Oil in Water (D O/W), Dispersed Water in Oil (D W/O), Transition Flow (TF), Very Fine Dispersed Oil in Water (VFD O/W) and a new flow pattern called Dispersed Oil Slug & Water in Water (D OS& W/W). The pressure fluctuation signals were also measured by a static pressure sensor and decomposed at five levels using wavelet transform. Then, standard deviation values of decomposition levels were used as input parameters of a Probabilistic Neural Network (PNN) to train the network for predicting the flow patterns. In addition, some considered numerical values for actual flow patterns together with a signal energy value of each level were used as input parameters of a MultiLayer Perceptron (MLP) network to estimate the oil holdup. The results indicated good accuracy for recognition of the flow patterns (accuracy of 100% and 95.8% for training data and testing data, respectively) and oil holdup (AAPE=9.6%, R=0.984 for training data and AAPE=8.07%, R=0.99 for testing data).*

**KEYWORDS:** *Vertical liquid-liquid flow; Two–phase flow; Oil holdup; Flow pattern; Pressure fluctuations; Wavelet transform; Artificial neural networks.*

## INTRODUCTION

Oil--water two-phase flows exist widely in petroleum and chemical industries, such as well bores, sub-sea pipelines and related equipment in oil field. To better understand the hydrodynamics of the liquid-liquid two-phase flow, its main parameters must be known. Flow pattern and oil holdup are two of the most important parameters that play a great role in the design and operation of oil-water flow systems. Depending on the mixture velocity, two-phase flow can acquire the various spatial distributions in pipes. These different configurations are known as flow pattern. Oil holdup is also defined as the fraction of pipe occupied by the oil phase. Generally, in multiphase flows, each phase flows at a different velocity and so, the holdup (in situ volume fraction)

* *To whom correspondence should be addressed.*
+ *E-mail: hakar@mail.yu.ac.ir*
*1021-9986/2017/2/125-141* *17/$/6.70*

of each phase is different from its input volume fraction [1]. Holdup and flow pattern are crucial parameters for predicting pressure drop, heat transfer, density and viscosity of mixture, corrosion rates in oil–water flow and relative averaged velocity of each phase.

Most studies of liquid–liquid two–phase flow have been performed for horizontal pipe orientations whereas little attention is paid to the vertical two–phase flow. *Govier et al.* [2] observed four different flow patterns in upward vertical oil–water two-phase flow in a 2.64 cm Inner Diameter (ID) pipe, i.e., drops of oil in water, slug of oil in water, water froth and water drops in oil. *Flores et al.* [3] carried out their experiments with vertical oil–water flow in a 5 cm ID pipe. They reported six kinds of flow patterns; dispersion oil–in–water flow, very fine dispersion oil–in–water flow and oil–in–water churn flow, water–in–oil churn flow, dispersion water–in–oil flow and very fine dispersion water–in–oil flow. *Jana et al.* [4] reported the flow patterns of dispersed bubbly flow, bubbly flow, churn–turbulent flow and core–annular flow for an upward oil–water flow in a 2.54 cm ID pipe. *Du et al.* [5] investigated vertical upward oil–water two–phase flow in a 2 cm ID pipe. They obtained five flow patterns using mini–conductance probes, i.e., very fine dispersed oil–in–water flow, dispersed oil–in–water flow, oil–in–water slug flow and water–in–oil and transition flow. *Mydlarz–Gabryk et al.* [6] identified flow patterns and measured holdup during oil–water two–phase flow through a vertical pipe with the ID of 3 cm. They classified the flow patterns in three categories: one with the dominant oil phase, a transitory area and one with the dominant water phase. They also compared the results of holdup measurements with the predictions from various void fraction models and correlations of gas–liquid flows.

Several methods have been proposed for determination of the flow pattern and holdup in two–phase systems. Commonly used methods for predicting the flow patterns are Positron Emission Tomography (PET) [7,8], Magnetic Resonant Imaging (MRI) [9-11], X-ray and γ–ray tomography [12,13], ultrasound tomography [14,15], electrical tomography [16, 17] and wire-mesh sensors [18,19]. The most commonly employed method for determination of liquid–liquid flow patterns is to visualize the flow in a transparent channel or through a transparent window on the wall of the pipe. In some cases, to better recognize, high–speed photography/video is may be employed to view through a transparent pipe wall particularly for high mixture velocities. Also, commonly used methods to measure the holdup are Quick Closing Valves (QCVs), *X*–, γ– and β–ray attenuation [20–23], wire mesh sensors [24,25], ultrasonic probes [26,27] and electrical probes [16, 28–33].

Each method mentioned above has its drawbacks. For example, nuclear sensors (*γ*–, *β*–, *X*–rays attenuation) are expensive and require safety conditions difficult to guarantee. In wire–mesh sensors method, by increasing the flow rates, the wires diameter should be increased with significant effects on the flow behavior [32]. Ultrasonic probes was found be useful only for oil holdup lower than 35% [26]. Electrical probes are affected salinity and conductivity property of the fluids. QCVs technique has been commonly employed in two–phase flow studies to exactly measure the holdup. But this method is inappropriate if continuous measurements are needed. It is often used for calibrating or comparison of measurements obtained from other methods.

Likewise, some researchers proposed the prediction of the flow pattern or holdup in two–phase flow using fluctuation signals obtained from different methods. *Shang et al.* [34] applied the wavelet signal extraction method to study the instability of two–phase flow and got the oscillation periods of mass flux conveniently, without frequency transfer. *Jana et al.* [4] analyzed the normalized time series data of a parallel wire type probe to identify the flow patterns during liquid–liquid two–phase flow through a vertical pipe by using Probability Density Function (PDF) and wavelet transform. *Zhen & Hassan* [35] employed the Particle Image Velocimetry (PIV) and wavelet auto–correlation methods to investigate two–dimensional full–field velocity components in the streamwise direction near–wall normal plane. *Chakrabarti et al.* [36] used an optical probe based on the difference in optical properties of two liquids during the simultaneous flow of two immiscible liquids through a horizontal conduit to characterize the different flow patterns. They quantified the probe signals using the moments of the PDF and the wavelet analysis. *Zong & Jin*. [37] analyzed and classified conductance signals of inclined oil–water flows into water dominated counter flow and transition flow pattern using wavelet analysis. *Nguyen et al.* [38] used the wavelet analysis technique for flow pattern

identification of vertical upward gas–liquid flow by using the void fraction signals obtained from a multi-channel Impedance Void Meter (IVM). *Tan et al.* [39] studied the flow structure of horizontal oil–water two–phase flow using a combined sensor. They measured the water holdup by combined conductivity and capacitance electrodes to deal with the water– and oil–continuous flow separately. They decomposed water holdup fluctuations with Continuous Wavelet Transform (CWT) and calculated a matrix of Local Wavelet Energy (LWE) coefficients at different decomposition scale for each experimental condition. The local flow structures and fluctuations of each typical flow pattern were characterized in a LWE coefficient map.

It is very interest to determine the flow pattern and the holdup from the pressure fluctuations, because the pressure sensors are robust, non–intrusive, inexpensive, well developed, unaffected by fluid salinity, readily available to a large range of operational pressure and temperature, resistant to most of fluids and fulfill most of the operational safety regulations [25, 40–42]. For this reason, some investigators attempted to predict the two–phase flow pattern or holdup from fluctuation signals of wall pressure [43–45] or differential pressure [46–49] using different plots and statistical moments of Probability Density Function (PDF) and wavelet transform. *Matsui* [46] estimated the flow patterns of nitrogen gas–water mixtures in a vertical pipe using statistical properties (PDF) of differential pressure fluctuations. *Elperin & Klochko* [47] proposed a wavelet transform–based method to analyze the time series of differential pressure fluctuations measured in a vertically installed venturi meter to identify flow regimes in two–phase gas–liquid flow. *Park et al.* [44] proposed the wavelet transform for identification of bed properties in a pressurized bubble column the fluctuating pressure signals. *Yang & Leu* [45] studied the transition velocities of Fluid Cracking Catalyst (FCC) in circulating fluidized bed systems by using statistical analysis and multi–resolution analysis of wavelet transformation on pressure fluctuation signals. *Sun et al.* [48] reported a flow–pattern map to distinguish the gas–liquid flow patterns in horizontal pipes based on the wavelet packet energy entropy of vortex–induced pressure fluctuation generated by a triangular bluff body perpendicular to the flow direction. *Han et al.* [42] combined the differential pressure method and conductance method to measure the water holdup of oil–water two–phase flow with low velocity and high water–cut through differential pressure method. They reported that when water holdup is less than 90%, with the oil–cut increasing, the slip effect between phases becomes more severe and flow structure of D O/W becomes more complex and so the prediction deviation of water holdup is high.

Due to the inherent complexity of two–phase flows, the interpretation of the pressure fluctuation signals to determine the respective flow pattern or the oil holdup is too difficult, particularly for liquid–liquid flows. Compared with gas–liquid systems, in liquid–liquid systems the density and viscosity difference between the phases is relatively low [49] and therefore pressure signal analysis is much more difficult. For either modeling phenomena which are too difficult to model from fundamental principles, or reduce the computational time for predicting expected behavior, Artificial Neural Network (ANN) techniques have been suggested as a powerful computational tool. *Marseguerra et al.* [50], *Cai et al.* [51] and *Antonopoulos–Domis & Tambouratzis* [52] were among the first researchers to use artificial neural network to better take advantage of the signals of complex phenomena. *Marseguerra et al.* [50] proposed the use of neural networks to the solution of problems in nuclear reactor physics with multiple signals as input and output data. *Cai et al.* [51] used the statistical moments acquired from pressure fluctuations in gas–liquid two–phase horizontal flow as input variables of Kohonen Self–Organizing feature Map (SOM) and divided them into four flow pattern. Antonopoulos–Domis and *Tambouratzis* [52] employed Artificial Neural Networks (ANN) for the on–line localization of a source of Even Plutonium Isotopes (EPI) material contained in sealed tanks. The ANN was trained on data obtained from a simulation of a well counter (filtered and Fourier transformed signals of the neutron detectors surrounding the well counter) for known positions of the EPI. Thereafter, a number of researchers employed the ANNs to predict the flow pattern or phase fraction of two–phase flows using fluctuation signals obtained from different methods. *Xie et al.* [53] trained two MultiLayer Perceptron (MLP) networks with two different outputs using the parameters of wall pressure signals to recognize the flow pattern of gas–liquid–pulp vertical three–phase flow. *Rosa et al.* [41]

used fluctuation signals of electrical resistivity probe in vertical gas–liquid flow to render first four statistical moments and its PDF as objective flow pattern indicators. *Peng & Yin* [54] proposed a method based on Electrical Capacitance Tomography (ECT) and an improved Least Squares Support Vector Machine (LS–SVM) for void fraction measurement of oil–gas two–phase flow. They employed the MLP network, Radial Basis Functions (RBF) and Probabilistic Neural Network (PNN). *Salgado et al.* [55] proposed a methodology for flow regimes identification and volume fraction predictions in water–gas–oil multiphase systems based on gamma–ray Pulse Height Distributions (PHDs) pattern recognition by means four Artificial Neural Networks (ANNs). The first ANN was trained to identify the dominant flow regime and the other three ones were trained for volume fraction predictions of each specifically regime. *Zhang et al.* [56] measured oil holdup of oil–water two–phase flow using thermocouple based on the thermal method. They proposed a model based on least square support vector machines and multi–wavelet transform of the temperature signal to forecast. *Bin & Hong* [57] proposed a gas–liquid two–phase flow regime identification method based on wavelet packet energy feature and Probabilistic Neural Network (PNN) according to the non–stationary characteristics of differential pressure fluctuation signals. *Nazemi et al.* [58] measured the void fraction percentage of two–phase flow regime using a g–ray attenuation technique and an MLP neural network with registered counts and transmitted detectors as its inputs and the void fraction percentage as its output. For a review of recent investigations on the applications of ANNs for predicting the main parameters of two–phase flow systems, such as flow pattern, void fraction, pressure drop, etc., see *Cong et al.* [59].

In this study, we experimentally investigate vertical upward liquid-liquid flow in a 2.54 cm ID pipe. Flow patterns and respective flow pattern map are determined using high speed photography. Oil holdup is measured by quick closing valves and static gauge pressure fluctuation signals are also acquired using a pressure sensor. Finally, we attempt to relate the acquired pressure fluctuations to the flow patterns and oil holdup with the help of wavelet transform and artificial neural network.

## EXPERIMENTAL SECTION

### *Experimental setup*

A schematic view of the flow loop experimental system is shown in Fig. 1.

All experiments were conducted at atmospheric outlet pressure and room–temperature. Water and diesel fuel (density=798 kg/m$^3$, viscosity=2.51 mPa.s and interfacial tension=37 mN/m) were selected as two immiscible liquids. Water and oil were pumped from their respective storage tanks (capacity=0.5 m$^3$) to mixing chamber via two centrifugal pumps (1 Hp, 100 L/min), after being pumped through previously calibrated flowmeters. The oil–water mixture entered into a vertical test section pipe and then proceeded to separator tank (capacity=1 m$^3$) where water was separated from oil by gravity and then both liquids returned to their respective storage tank. The Inner Diameter (ID) and the length of the test section were 2.54 cm and 1.5 m, respectively and the length of pipe between the mixing chamber outlet and the entrance of the test section was selected 2 m to ensure fully developed the flow pattern. Also, a transparent acrylic pipe was selected as the test section to enable visual observation of the flow phenomena. A pressure sensor (IFM electronic sensors) connected to tapping in the test section at a distance of 2.3 m from the vertical pipe inlet was applied to measure the static gauge pressure fluctuations (in mbar). The sampling frequency was 20 Hz for duration of 100 s. In order to minimize the probable effects of mechanical vibration on pressure fluctuations, the sensor was connected to the test section. The oil holdup was measured using QCV technique and the flow patterns were identified by a digital high–speed photography (Nikon, COOLPIXP 500). Because diesel fuel is a liquid transparent and its color is different from the water, it provides the possibility of flow pattern accurate diagnosis through photography. The superficial velocities of water ($U_{sw}$) and oil ($U_{so}$) were varied 0.14–1.36 and 0.057–0.85 m/s, respectively, and a total of 60 experimental test were conducted under mentioned conditions. During each experiment the water velocity was kept constant and the oil velocity was gradually increased. In order to ensure the reproducibility of the results, the entire experiments were repeated at least twice. In each run, the pressure fluctuation signals were recorded by a data logger and shown in computer using the LABVIEW software installed and programmed for this purpose.

## OBSERVED FLOW PATTERNS

Five different flow patterns were identified aided by digital high speed photographs as follows: Dispersed oil

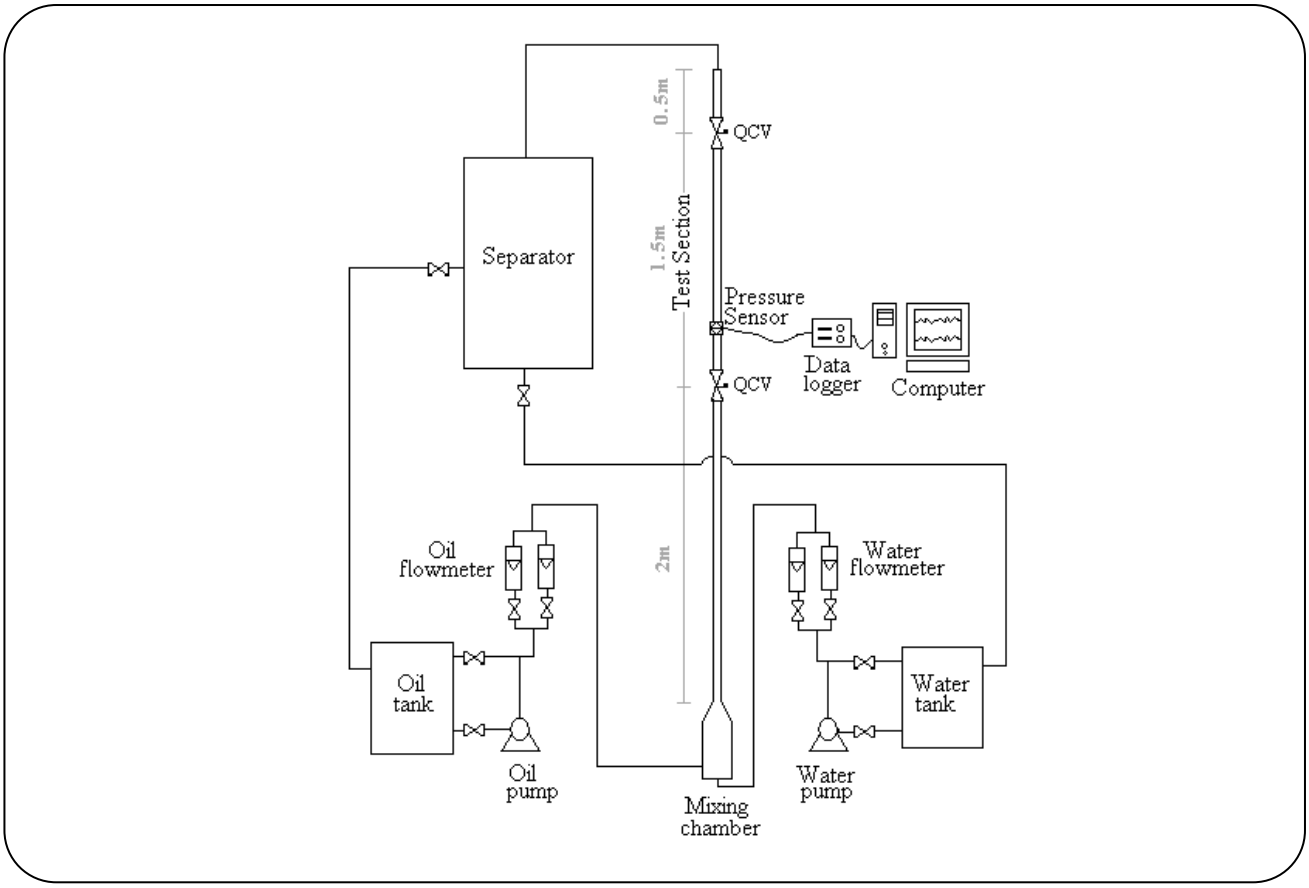


***Fig. 1: Schematic view of the oil–water flow loop.***

Slug & Water in Water (D OS & W/W), Dispersed Oil in Water (D O/W), Dispersed Water in Oil (D W/O), churn or Transition Flow (TF) and Very Fine Dispersed Oil in Water (VFD O/W). Photographs of the flow patterns are shown in Fig. 2 and the experimental flow pattern map is shown Fig. 3, in which $U_{sw}$ and $U_{so}$ represent water and oil superficial velocity, respectively.

Among the 60 runs performed, the flow patterns of D OS & W/W, D O/W, D W/O, TF and VFD O/W were observed 2, 32, 4, 4 and 18 times, respectively. Dispersed Oil Slug and Water in Water (D OS & W/W) flow pattern occurred at low oil–water mixture velocity (Figs. 2a and 3). Under this situation, some transparent bubbles, marked by black circles, as well as a large oil bubbles were observed in water continuous phase. Because after closing the QCVs, no air was seen in the test section pipe, so it ensured that air does not leak into the system. Therefore these transparent bubbles must be water phase that was trapped by a relatively resistant surface caused by interfacial tension between oil and water. Perhaps theses bubbles (water drops) were at first within the oil phase and then, they was separated from it because of the density difference, and due to the previous contact of water drop surface with the oil, a relatively resistant layer formed on the its surface due to the interfacial tension. Such bubbles may be affective in increasing the pressure drop and may be seen in three–layer flow pattern of horizontal liquid–liquid flows. At higher mixture velocity the Dispersed Oil in Water (D O/W) flow pattern was observed where oil phase was dispersed as bubbles in water continuous phase (see Fig. 2b). The Dispersed Water in Oil (D W/O) flow pattern was observed at high superficial velocity of oil (see Fig. 2c). In this flow pattern, turbulence energy of oil phase was high enough to disperse the water as drops in oil continuous phase. In the transition (TF) or churn flow pattern that often occurs at a certain range of the oil or water holdup, both liquid phases alternately appeared as continuous phase (see Fig. 2d). This flow pattern is a transition state between the water continuous and oil continuous flow pattern. When

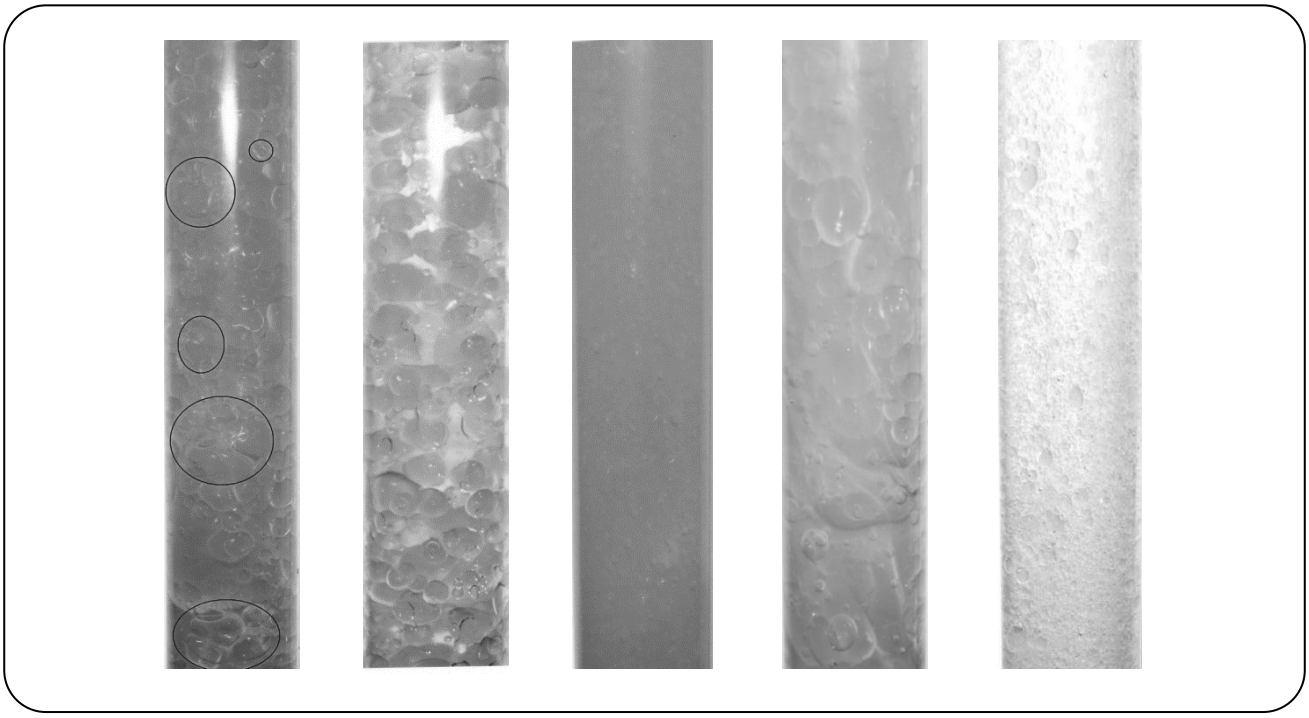

***Fig. 2: Photographs of flow patterns in vertical upward oil–water two phase flow.***

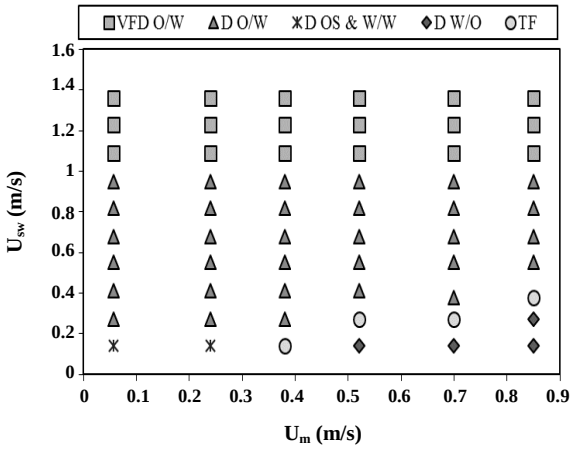


***Fig. 3: Experimental flow pattern map.***

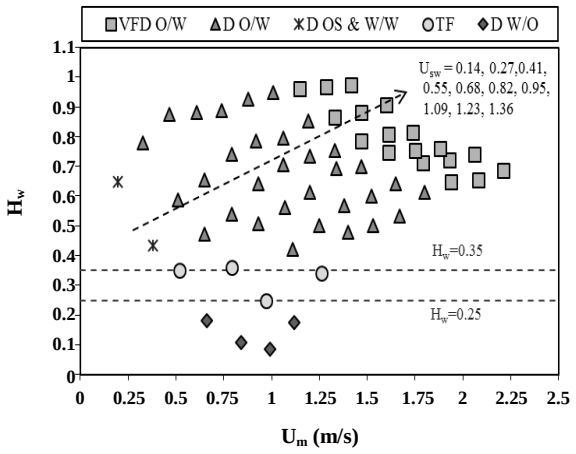


***Fig. 4: Flow pattern map based on water holdup and mixture velocity.***

the superficial velocity of water was very high (1.09–1.36 m/s), oil phase was broken into very small droplets in water continuous phase. This flow pattern was called Very Fine Dispersed Oil in Water (VFD O/W) flow (see Fig. 2e).

***Oil hodup measurement***

As mentioned earlier, the oil (and water) holdup was measured by quick closing valves. The experimental results based on water holdup and mixture velocity are shown in Fig. 4.

These results confirm the proposed transition criteria by *Du et al.* [5] for oil and water dominant flow pattern boundaries mentioned in the literature review. They stated that the transition is affected from the water holdup. They proposed that transition to oil dominant flow pattern and transition to water dominant flow pattern often happens at water holdup $H_w$=0.25 and $H_w$=0.35, respectively. Fig. 5 compares in situ oil fraction (oil holdup, $H_O$) against the inlet oil volume fraction ($\beta_o$) at all of the used mixture velocities.

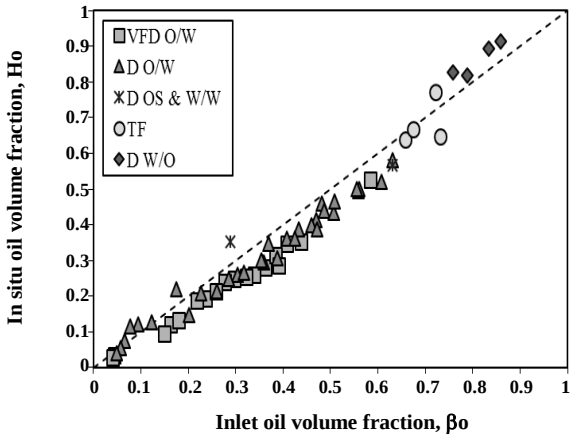


***Fig. 5: In situ oil holdup against inlet oil volume fraction.***

The difference between in situ oil holdup and inlet oil fraction indicates that there exists a slip velocity between two liquids due to the different properties of them. In most of the cases (range of $\beta_o$ = 0.15–0.75) the inlet oil fraction is less than the oil holdup.

***Pressure fluctuation signals***

A typical of the recorded pressure signals for each flow pattern is shown in Fig. 6.

As mentioned earlier, the signals were sampled at 20 Hz during 100 s. Although in the liquid–liquid flow system, due to its incompressible property the mechanical, vibration is negligible, however, to ensure that the pressure fluctuations would be caused only by the hydrodynamic nature of the two–phase flow, two centrifugal pumps were used for both liquids and special supports were designed in order to satisfy the dynamic neutrality (hydrodynamic forces don not generate mechanical vibrations). In this study, owing to the random and complex nature of the recorded pressure fluctuation signals and therefore difficulty of predicting the flow patterns and oil holdup, wavelet transform and artificial neural network were utilized to overcome this difficulty.

***Wavelet transform***

Wavelet Transform (WT) analysis is a very powerful time–frequency tool for analysis of transitory and non–stationary signals. Unlike the short time Fourier transform method that suffers from a limitation due to a fixed resolution in both time and frequency, WT is a more flexible method of time–frequency representation of a signal by allowing the use of variable sized windows. In WT, to get precise time resolution, narrow windows are used at high frequencies (corresponding to small scales), while to get finer frequency resolution, wide windows are utilized at low frequencies (corresponding to large scales). Two different kinds of wavelet transform can be distinguished, Continuous Wavelet Transform (CWT) and Discrete Wavelet Transform (DWT). CWT performs a Multi–Resolution Analysis (MRA) by contraction and dilatation of the wavelet functions, whereas DWT uses filter banks for the construction of the multi–resolution time–frequency plane.

***Wavelet decomposition of pressure fluctuation signals***

There are different families of wavelet functions, such as Harr, Daubechies, Maxican hat, and Splines wavelets. Since the Daubechies wavelets [60,61] are compactly supported orthogonal wavelets with external phase and highest number of vanishing moments for a given support width, they have frequently been used in multiphase systems to decompose the time–series signals. In this work, Daubechies 4 (Db4) wavelet with 5 levels was chosen for the analyzing wavelet. For all wavelet analysis, Matlab Wavelet Toolbox environment with wavelet toolbox was utilized. Wavelet analysis of a typical of signal obtained from pressure sensor is shown in Fig. 7 where $d_1$ (detail coefficient of the level 1) and $a_5$ (approximation coefficient of the level 5) represent the highest and lowest frequency bands, respectively, and $d_2$–$d_4$, reflect progressively lower frequency bands.

For a compact and complete representation [62], the results were presented as the standard deviation at the different levels of details ($d_1$–$d_5$) and approximation ($a_5$) for each signal. Standard Deviation (SD) is a measure of scattering of the distribution around the mean value and given as:

$$SD = \sqrt{\frac{1}{n-1}\sum_{i=1}^{n}\left(x_i - \mu\right)^2} \qquad (1)$$

Where $n$ is total of all points, $x_i$ is signal values from $i$ = 1 until $n$–1 and $\mu$ is mean value of the signal.

The plots of details and approximation levels vs. their standard deviation exhibit special plots for each flow pattern. Fig. 8 shows the plots created by plotting

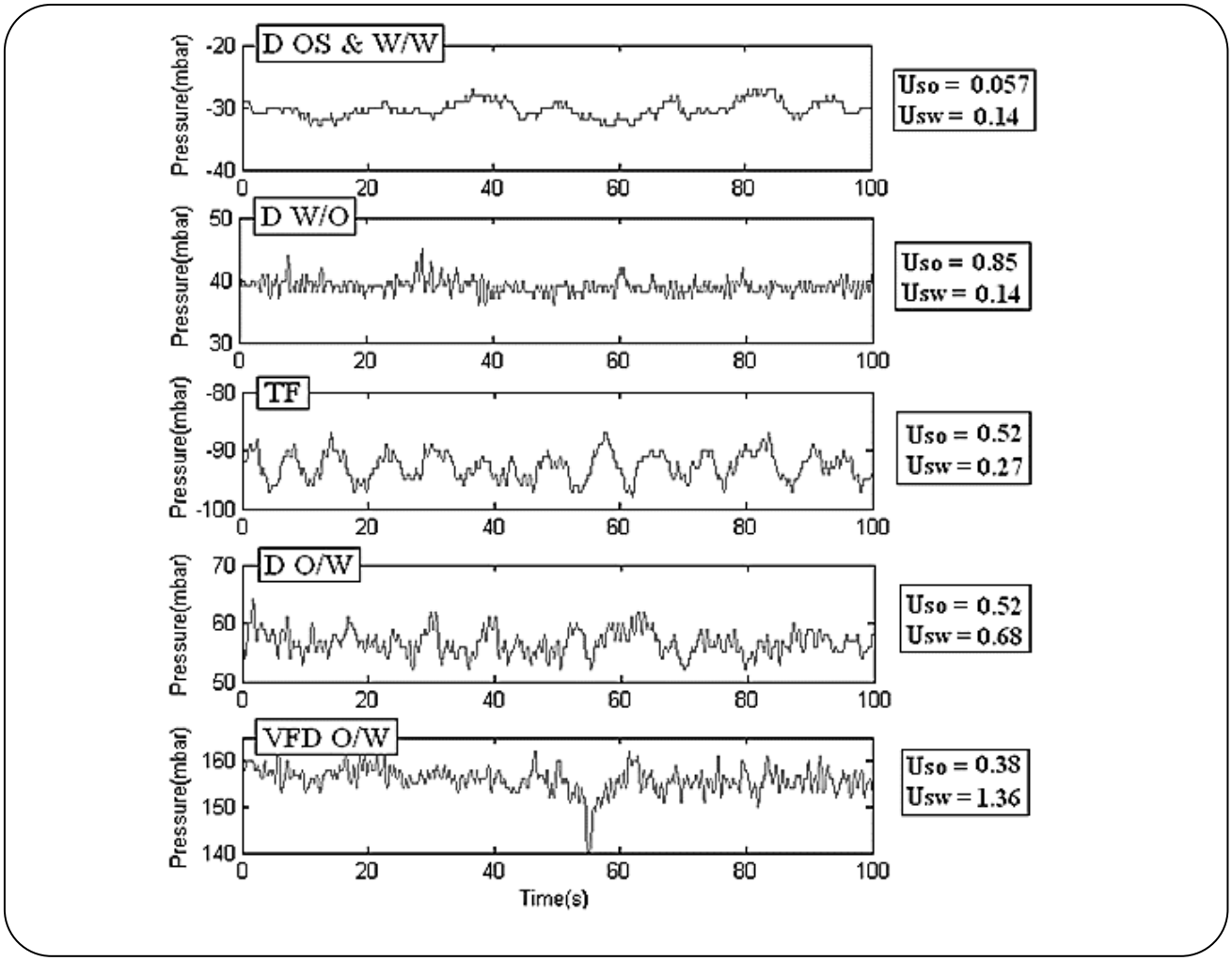


***Fig. 6: Typical of time series of pressure fluctuation signals in observed flow patterns.***

the standard deviations of details and approximation coefficients at different decomposition levels for D O/W flow pattern.

These plots can be divided into three groups. The first group is based on the lower oil holdup of 0.2, where the standard deviation has a peak at $d_3$ and slope change is negative between the $d_4$ and $d_5$. The second group is based on the oil holdup of 0.2 to the lower oil holdup of 0.4, where the standard deviation has a peak at $d_3$ similar to the first group, but, in this case the slope change between $d_4$ and $d_5$ is positive. Finally, the third group is related to the higher oil holdup of 0.4, where the standard deviation increases from $d_1$ to $d_5$ but drops down at $a_5$.

Standard deviation of the details and approximation coefficients at different resolution levels are also plotted for the VFD O/W flow pattern in Fig. 9. Although it seems that the plots of this figure are similar to the first or the second group related to the D O/W flow pattern, but in this figure, the difference between $d_2$ and $d_4$ is lower and the plots between $d_2$ and $d_4$ are almost asymmetry.

The plots of standard deviations of different resolution levels related to D W/O are plotted in Fig. 10. These plots can be discriminated probably from the previous flow patterns plots by oscillations of values of the standard deviation from $d_1$ to $d_5$ close to 0.5.

Fig. 11 shows the plots of the standard deviations of details and approximation coefficients at different resolution levels related to D OS W/W flow pattern**.** Similar trends can be seen for variation of values of the standard deviation of coefficients as standard deviation increases gradually from $d_1$ to $d_5$ but then $d_5$ increases sharply to $a_5$.

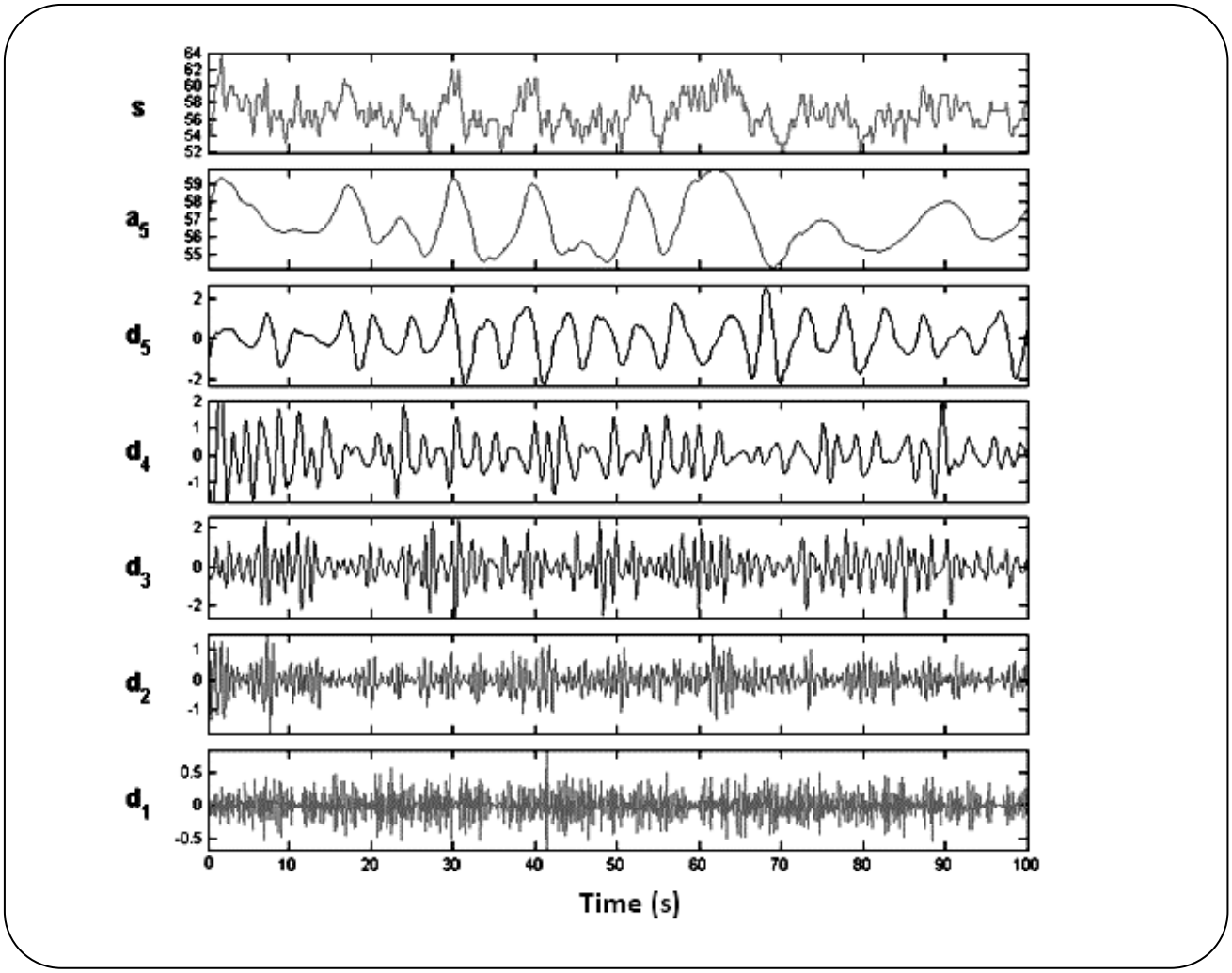


***Fig. 7: Wavelet analysis of a typical pressure fluctuation signal for DO/W flow pattern ($U_{so}$ = 0.52, $U_{sw}$ = 0.68).***

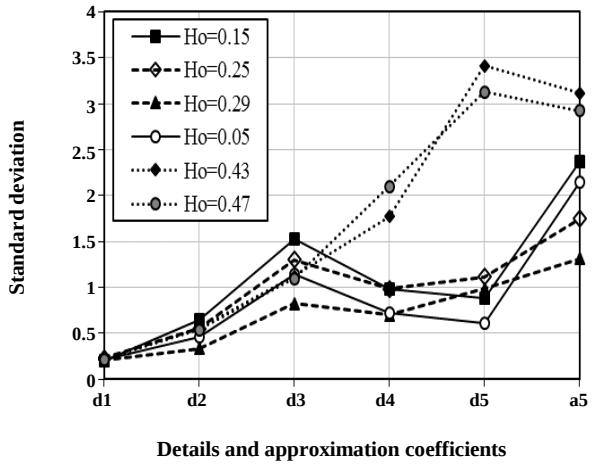


***Fig. 8: Typical of plots of standard deviations of details (d1–d5) and approximation coefficients at different resolution levels for D O/W flow pattern.***

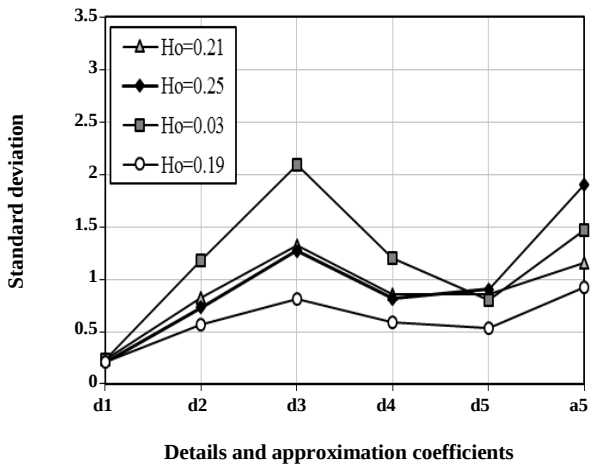


***Fig. 9: Typical of plots of standard deviations of details (d1–d5) and approximation coefficients at different resolution levels for VFD O/W flow pattern.***

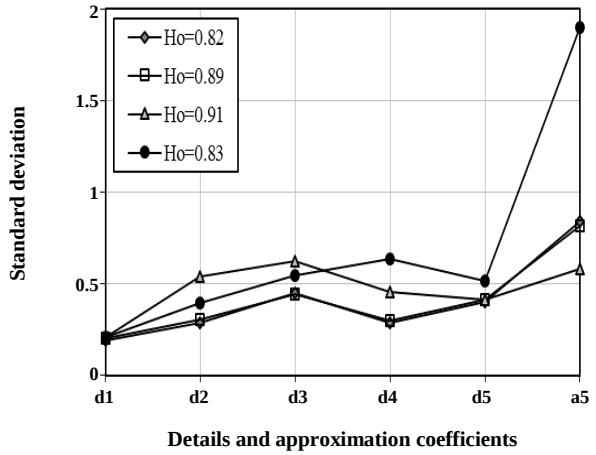


*Fig. 10: Plots of standard deviations of details (d1–d5) and approximation coefficients at different resolution levels for D W/O flow pattern.*

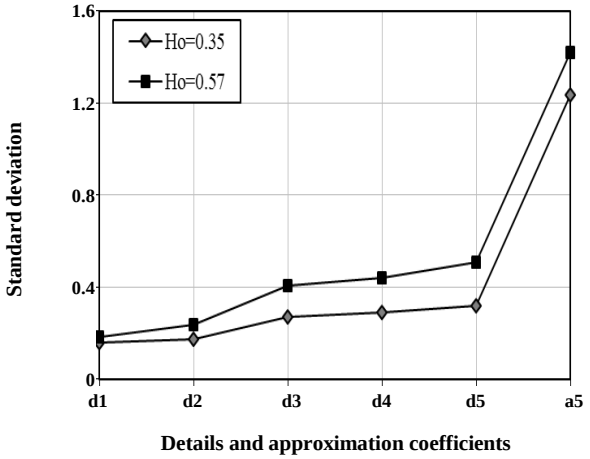


*Fig. 11: Plots of standard deviations of details (d1–d5) and approximation coefficients at different resolution levels for D OS & W/W flow pattern.*

Finally, the plots of different resolution levels against their standard deviations related to the flow pattern of TF are plotted in Fig. 12. As can be seen, the standard deviation of coefficients increases entirely from $d_1$ to $a_5$, and unlike the D OS & W/W flow pattern, the standard deviation dose not increases sharply from $d_4$ to $a_5$.

Although the flow pattern and in some cases the range of oil holdup can be predicted using the above method, it is difficult to recognize the flow pattern in some cases due to the relative similarity of the plots of a flow pattern with the other flow pattern plots. Moreover, the predicted oil holdup should be close to the actual oil holdup. For this reason, in addition to wavelet transform, Artificial Neural Network (ANN) were used to predict the flow pattern and the oil holdup.

## ARTIFICIAL NEURAL NETWORK (ANN)

Artificial Neural Network (ANN) is a mathematical or computational model based on biological neural networks that contains of an interconnected group of artificial neurons and processes information using a connectionist approach to computation. ANNs extract the relationship between the input and output data and can be effectively used as excellent pattern classifiers [41] and for nonlinear systems where inputs and outputs have complex relationships [63–65]. A multilayer network has commonly one input layer, one output layer and one or more hidden layers. Kohonen Self–Organizing Feature Map (SOM), MultiLayer Perceptron (MLP) with Feed-Forward Back–Propagation (FFBP) training algorithm, Radial Basis Function (RBF), Probabilistic Neural Network (PNN) and Learning Vector Quantization (LVQ) are commonly used networks for classification. In this study, the PNN was selected to classify the flow patterns using pressure fluctuation signals because of its high speed in operation and high accuracy in pattern identification [66].

## FLOW PATTERN AND OIL HOLDUP PREDICTION USING WT AND ANN

### *Flow pattern prediction using WT and PNN*

The PNN based on the Bayes–Parzen classification theory was developed by *Specht* [67]. It estimates a PDF for each data class based on the training set data and an optimized spread constant ($\sigma$), and is composed of four layers namely input layer, pattern (hidden) layer, summation layer and decision (output) layer. The pattern layer contains one neuron (node) for each training case available, and on receiving the outputs of input layer, calculates an Euclidean distance measure between the presented input vector and the training example represented by that pattern neuron at each neuron and then processed through a Gaussian activation function as

$$\Phi_j(x) = \exp\left(\frac{\left\|x - \bar{x}_j\right\|}{2\sigma_j^2}\right) \quad (2)$$

Where $x$ and $x_j$ are the vector of random variables and the $j$th training vector, respectively. The summation layer computes the summation of the outputs of the hidden

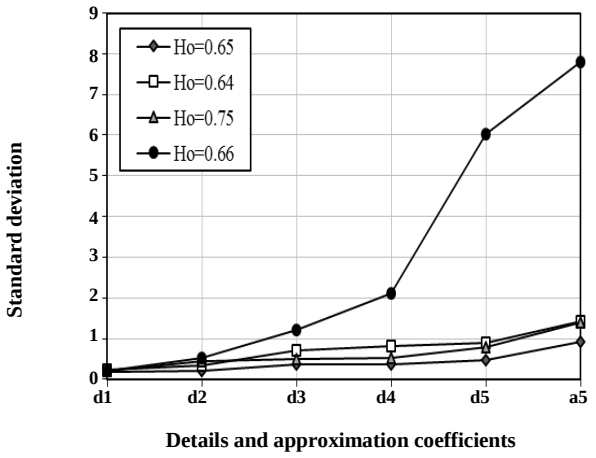


***Fig. 12: Plots of standard deviations of details (d1–d5) and approximation coefficients at different resolution levels for TF flow pattern.***

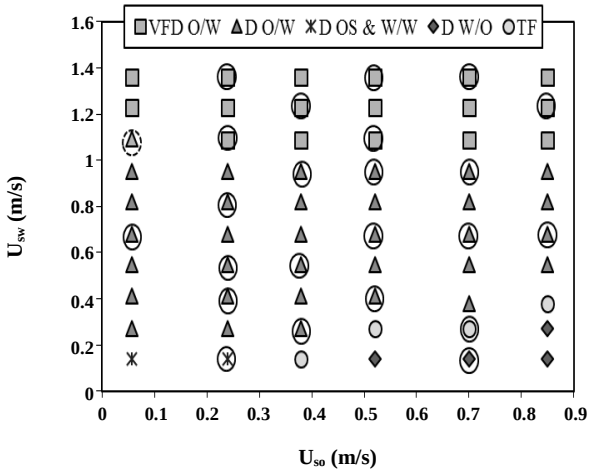


***Fig. 13: Predicted flow pattern map by PNN network.***

layer for each respective data class. Then, the outputs of the summation neurons are compared and the largest of them is fed forward to the decision layer to yield the computed class and the probability that this example will belong to that class. Only one variable, spread constant ($\sigma$), needs to be altered for this architecture to obtain an optimal PNN. As the spread constant determines the shape of the Gaussian functions, selection of it is crucial.

In the present study, standard deviation values of the details and approximation coefficients are chosen as the inputs of PNN (six inputs). Some numerical values were considered for each flow pattern to make it comprehensible for PNN. The numerical values were from one to five for VFD O/W, D O/W, D OS & W/W, TF and D W/O flow patterns, respectively. 60% of data were used for training and the remainders were used for testing the network. These sets were chosen carefully, so that in training set enough data would be available for each flow pattern. To evaluate the network performance, Mean Squared Error (MSE) was used by the following equation:

$$\mathrm{MSE}=\frac{1}{\mathrm{n}}\sum_{\mathrm{i}=1}^{\mathrm{n}}\left(\mathrm{Y_i}-\mathrm{X_i}\right)^2 \qquad (3)$$

where $n$ is the number of all data, $Y_i$ is the actual values and $X_i$ is predicted values by the network. To find the best spread for Gaussian function, the network errors for different spreads were calculated, and using the trial and error method the minimum MSE of the test set was obtained by spread constant of 0.28. Flow pattern map predicted by the PNN is shown in Fig. 13 where the black circles are testing set points. As shown in this figure, the number of misidentification on testing set was only one marked by the dash line. As a result, percentage accuracy of PNN was obtained 95.8% for the testing set, while that was achieved 100% for the training set.

***Prediction of oil holdup using WT and MLP***

To be able the use a neural network model as a good function approximation (regression), MultiLayer Perceptron (MLP) which is most commonly used for fitting was selected. This network has an input layer, one or more hidden layers and an output layer in which each layer comprise a number of interconnected neurons. Each layer has some artificial neurons (nodes), a weight matrix (w), and an output vector, and each neuron in the hidden and output layer has a bias (b) and an activation function. In the present study, hyperbolic tangent sigmoid and linear activation functions were used in the hidden and output layers, respectively. Also, Levenberg–Marquardt back–propagation algorithm was used to adjust the weights and biases and minimize the difference between network output and target (training the network).

Although the standard deviation of the details and approximation coefficients of different decomposition levels were suitable parameter to recognize the flow pattern, in initial evaluations, the present authors found that the signal energy values of each level together with

***Table 1: The energy range (%) of coefficients at different decomposition levels for different flow patterns signals.***

| Coefficient energy | Flow pattern | | | | |
|---|---|---|---|---|---|
| | D OS & W/W | D O/W | D W/O | TF | VFD O/W |
| $Ea_5$ | 99.995 – 99.999 | 99.942 – 99.998 | 99.993 – 99.997 | 99.926 – 99.995 | 99.927 – 99.999 |
| $Ed_5$ | 0.0001 – 0.0002 | 0.00006 – 0.0007 | 0.0001 – 0.0005 | 0.0001 – 0.0005 | 0.00002 – 0.0012 |
| $Ed_4$ | 0.0002 – 0.0004 | 0.0003 – 0.003 | 0.0004 – 0.001 | 0.0006 – 0.0009 | 0.00002 – 0.014 |
| $Ed_3$ | 0.0004 – 0.001 | 0.0009 – 0.012 | 0.0008 – 0.002 | 0.0009 – 0.003 | 0.00007 – 0.043 |
| $Ed_2$ | 0.0003 – 0.001 | 0.0007 – 0.012 | 0.0004 – 0.001 | 0.001 – 0.004 | 0.00005 – 0.011 |
| $Ed_1$ | 0.0004 – 0.002 | 0.002 – 0.018 | 0.0004 – 0.002 | 0.0023 – 0.06 | 0.00008 – 0.0065 |

the appropriated Flow Pattern Number (FPN) as the input parameters of the MLP network have superior performance to predict the oil holdup compared with the standard deviation values. Range of signal energy of different decomposition levels for different flow patterns is represented in Table 1.

As is shown this table, the approximation coefficients comprise most of the signals energy while the detail coefficients of $d_5$ have the lowest energy. To train the MLP network, the signal energy of different decomposition levels together with the actual Flow Pattern Number (FPN) were used as the input variables (7 input variables) while the target of the ANN was defined by the oil holdup values ($H_o$) measured by Quick Closing Valves (QCVs) technique. One of the main problems related to the training of the MLP is over–fitting or over–training where the trained network can only produce good prediction for known data set and it is unable to give reasonable prediction for a new data set [68]. In the present study, "early stopping" technique that is one of the most common methods to avoid over–fitting and improve generalization capability of the network [69] was applied. In this method, all of the data are divided into three subsets, namely training, validation and testing sets. The training set is employed to compute the gradient and updating the values of weights and biases, and the validation set is utilized to ensure the generalization of the developed network during the training process. When the validation error increases for a predetermined number of epochs, the training process is stopped and the testing set is used to verify the final performance of the network. So the test set is not applied during the training process and the validation set in only applied to stop the process of network training [70]. The proposed MLP was trained, validated and tested with randomly 70% (42 data points), 15% (9 data points), and 15% (9 data points), respectively. Correlation coefficient (R) and Mean Square Error (MSE) were used as the criterions for selecting the best network topology. Generation of initial values of the weights and biases and selection of the training data is performed randomly, and these random choices will affect the network performance. Likewise, the number of neurons in input and output layers is equal to the number of input and output variables, respectively, while the number of neurons in hidden layer is dependent upon the complexity of the problem and can significantly affect the final performance of the network. So, in each network training, the output may be different when the network is initialized. On the other hand, there is not a general rule for the determination of the optimal structure of MLP network and it is usually determined through the method of trial–and–error [71]. To determine the optimal number of neurons in the hidden layer, different structures of the network having different numbers of neurons in the hidden layer were employed to predict the oil holdup. The number of neurons in the hidden layer were varied from 1 to 15 and each network having a certain number of neurons was repeatedly run for 80 times (in a total of 1200 trails). In each trial, the network was trained with different random initial weights, biases and training data. Finally, the best network (having the best performance) was determined and its number of neurons in the hidden layer was selected as the optimal number of neurons [70]. The best performance (the minimum MSE) was obtained for 11 neurons in hidden layer (see Fig. 14).

The best performance of MLP network with 11 neurons in the hidden layer to describe the pressure gradient was validated by the correlation coefficient (R)

***Table 2: Performance evaluation of the trained MLP network for training, validation and testing of all data sets.***

| Data set | MSE | AAPE (%) | R | No. of data points |
|---|---|---|---|---|
| Train | 0.00153 | 9.60 | 0.984 | 42 |
| Validation | 0.00246 | 9.54 | 0.962 | 9 |
| Test | 0.00077 | 8.07 | 0.990 | 9 |
| All | 0.00160 | 9.33 | 0.983 | 60 |

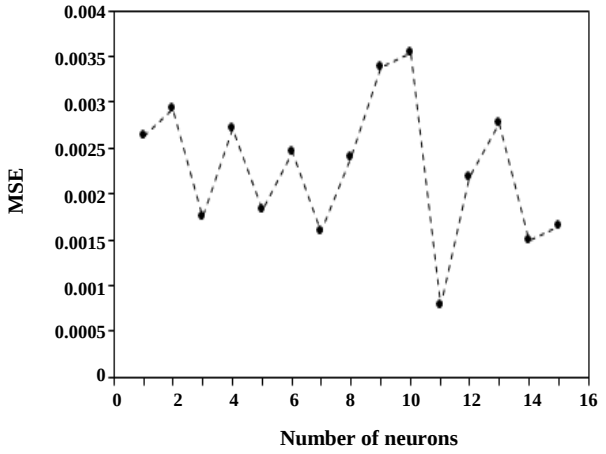


***Fig. 14: MSE of network for different number of neurons in hidden layer.***

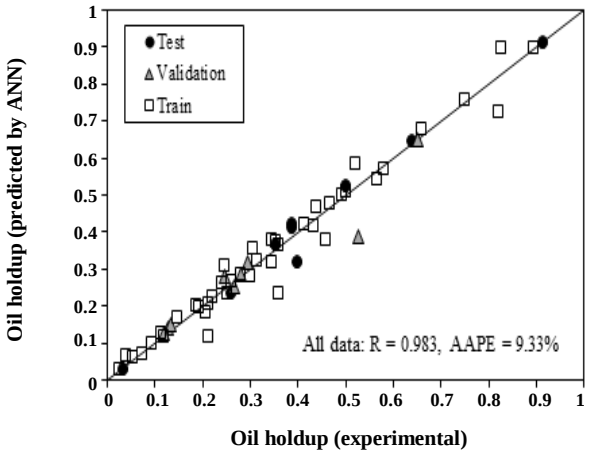


***Fig. 15: Comparison of oil holdup values predicted by ANN and measured by QCV.***

and Average Absolute Percent Error (AAPE) between the experimental and the predicted data from the network defined as:

$$AAPE = \frac{1}{n}\sum_{i=1}^{n}\left|\frac{Y_i - X_i}{Y_i}\right| \times 100 \quad (4)$$

$$R = \frac{\sum_{i=1}^{n}\left(Y_i - \bar{Y}\right)\left(X_i - \bar{X}\right)}{\sqrt{\sum_{i=1}^{n}\left(Y_i - \bar{Y}\right)^2\left(X_i - \bar{X}\right)^2}} \quad (5)$$

Where $\bar{Y}$ and $\bar{X}$ are the average of the experimental and predicted values, respectively. The details of ANN performance for all data sets are represented in Tables 2 and Fig. 15.

The accuracy between the neural network predictions and experimental data was achieved with AAPE of 9.6% and correlation coefficient (R) of 0.984 for training data set and AAPE of 8.07% and R value of 0.99 for testing data. The AAPE and R value for all data sets were also calculated as 9.33% and 0.983, respectively. These results show good fitting between the oil holdup experimental data and the predicted values by the proposed ANN model. As a result, by knowing the flow pattern, the oil holdup can be predicted from the pressure fluctuations.

In order to use the method proposed in the present paper, if the sampling frequency is more, less time is required and possibly better results will be obtained for predicting the flow pattern and oil holdup. If the flow pattern is unknown to use the trained MLP network and if the trained PNN can correctly predict all of the flow pattern, the PNN results (the predicted Flow Patter Number, FPN) can be used as an input variable of the trained MLP network to predict the oil holdup, as shown in Fig. 16.

In this figure, PNN and MLP are the trained networks as described previously. At first, the original signal is decomposed at 5 levels by using wavelet transform (Db4 wavelet). Then the standard deviation of the levels coefficients are used as input variables of the PNN to predict the Flow Pattern Number (FPN). Finally, the predicted FPN together with the signal energy of details and approximation coefficients of the levels are utilized as input variables of the MLP network to predict the oil holdup.

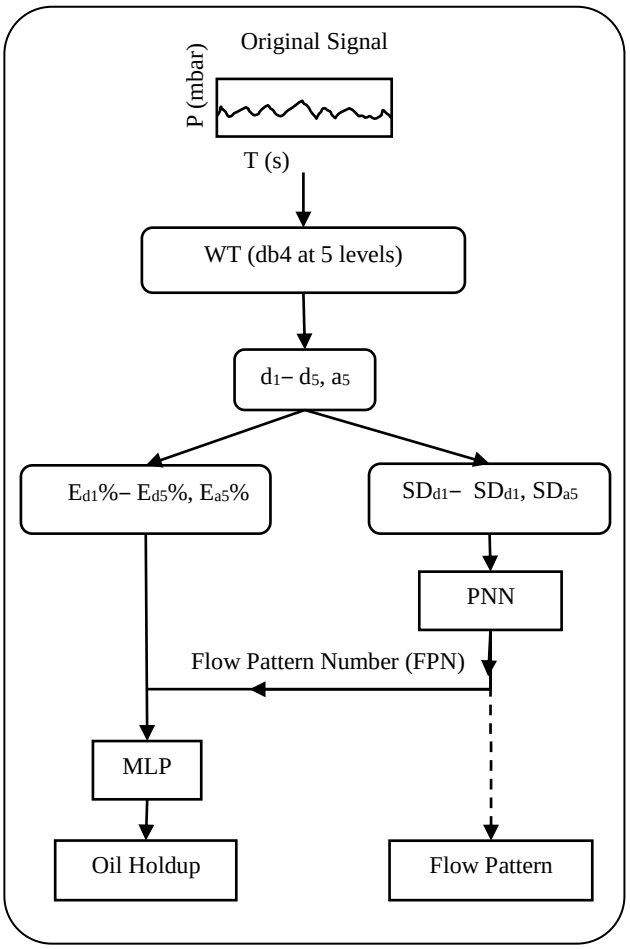


***Fig. 16: Process of proposed method for prediction of flow pattern and oil holdup using pressure fluctuation signals.***

## CONCLUSIONS

The flow pattern and the oil holdup were predicted successfully from the pressure fluctuation signals using wavelet transform and artificial neural network. For this purpose, the PNN and MLP networks were trained to predict the flow patterns and oil holdup, respectively. The results indicated that the proposed method can be a useful tool for characterizing the different vertical upward oil–water flow patterns (accuracy=95.8% for testing data) and determining the oil holdup (AAPE=8.07%, R=0.99 for testing data). As a result, flow pattern and oil holdup can be predicted for vertical oil–water two–phase flow using pressure fluctuation signals obtained by only one pressure sensor and with the help of wavelet transform and artificial neural network.

*Received : Jul. 24, 2014 ; Accepted : Aug. 22, 2016*

## REFERENCES

[1] Azizi S., Awad M.M., Ahmadloo E., Prediction of Water Holdup in Vertical and Inclined Oil–Water Two–Phase Flow Using Artificial Neural Network, *Int. J. Multiphase Flow*, **80**: 181–187 (2016).

[2] Govier G.W., Sullivan G.A., Wood R.K., The Upward Vertical Flow of Oil–Water Mixtures, *Can. J. Chem. Eng.*, **4**: 67–**75** (1961).

[3] Flores J.G., Chen X.T., Sarica C., Brill J.P., Characterization of Oil–Water Flow Patterns in Vertical and Deviated Wells, *SPE. Prod. Facil.*, **14**: 102–109 (1999).

[4] Jana K., Das G., Das P.K., Flow Regime Identification of Two–Phase Liquid–Liquid Upflow Through Vertical Pipe, *Chem. Eng. Sci.*, **61**: 1500–1515 (2006).

[5] Du M., Jin N.D., Gao Z.K, Wang Z.Y., Zhai L.S., Flow Pattern and Water Holdup Measurements of Vertical Upward Oil–Water Two–Phase Flow in Small Diameter Pipes, *Int. J. Multiphase Flow*, **41**: 91–105 (2012).

[6] Mydlarz–Gabryk K., Pietrzak M., Troniewski L., Study on Oil–Water Two–Phase Upflow in Vertical Pipes, J. *Petrol. Sci. Eng.*, **117**: 28–36 (2014).

[7] Parker D.J., McNeil P.A., Positron Emission Tomography for Process Applications, *Meas. Sci. Technol.*, **7**: 287–296 (1996).

[8] Bemrose C.R., Fowles P., Hawkesworth M.R., O'Dwyer M.A., Application of Positron Emission Tomography to Particulate Flow Measurement in Chemical Engineering Processes, *Nuclear. Instruments. Meth. A.*, **273**: 874–880 (1988).

[9] Mantle M.D., Sederman A.J., Dynamic MRI in Chemical Process and Reaction Engineering, *Prog. Nucl. Mag. Res. Sp.*, **43**(1): 3–60 (2003).

[10] Holland D.J., Müller C.R., Dennis J.S., Gladden L.F., Davidson J.F., Magnetic Resonance Studies of Fluidization Regimes, *Ind. Eng. Chem. Res.*, **49**. 5891–5899 (2010).

[11] Reyes Jr. J.N., Lafi A.Y., Saloner D., The Use of MRI to Quantify Multiphase Flow Patterns and Transitions: An Application to Horizontal Slug Flow, *Nucl. Eng. Des.*, **184**: 213–228 (1998).

[12] Bieberle M., Fischer F., Schleicher E., Hampel U., Koch D., Aktay K.S.C., Menz H.J., Mayer H.G., Ultrafast Limited–Angle–Type X–Ray Tomography, *Appl. Phys. Lett.*, **91**: 123516 (2007).

[13] Kumar S.B., Moslemian D., Duduković M., A γ–Ray Tomographic Scanner for Imaging Voidage Distribution in Two–Phase Flow Systems, *Flow. Meas. Instrum*., **6**(1): 61–73 (1995).

[14] Yang M., Schlaberg H.I., Hoyle B.S., Beck M.S., Lenn C., Real–Time Ultrasound Process Tomography for Two–Phase Flow Imaging Using a Reduced Number of Tansducers IEEE Transactions on Ultrasonics, *Ferr. Freq. Control*., **46**: 492–501 (1999).

[15] Liang F., Zheng H., Yu H., Sun Y., Gas–Liquid Two–Phase Flow Pattern Identification by Ultrasonic Echoes Reflected from the Inner Wall of a Pipe, *Meas. Sci. Technol.*, **27**(3): 035304 (2016).

[16] Geraets J.J.M., Borst J.C., A Capacitance Sensor for Two–Phase Void Fraction Measurement and Flow Pattern Identification, *Int. J. Multiphase Flow*, **14**: 305–320 (1988).

[17] Xie C.G., Reinecke N., Beck M.S, Mewes D., Williams R.A., Electrical Tomography Techniques for Process Engineering Applications, *Chem. Eng. J*., **56**: 127–133 (1995).

[18] Prasser H.M., Böttger A., Zschau J., A New Electrode–Mesh Tomograph for Gas–Liquid Flows, *Flow. Meas. Instrum*., **9**: 111–119 (1998).

[19] Liu W., Tan C., Dong F., A Wire–Mesh Sensor for Air–Water Two–Phase Flow Imaging, IEEE "International Instrumentation and Measurement Technology Conference (I2MTC) Proceedings", 364–369 (2015).

[20] Smith A.V., Transient Density Measurements in Two–Phase Flows Using X–Rays, *J. Br. Nucl. Energy Soc.*, **10**: 99–106 (1971).

[21] Eberle C.S., Lenug W.H., Ishii M., Revankar S.T., Optimization of a One–Shot Gamma Densitometer for Measuring Area–Averaged Void Fractions of Gas–Liquid Flows in Narrow Pipelines, *Meas. Sci. Technol.*, **5**: 1146–1158 (1994).

[22] Luggar R.D., Key M.J., Morton E.J., Gilboy W.B., Energy Dispersive X–Ray Scatter for Measurement of Oil–Water Ratios, *Nucl. Instrum. Meth. A.*, **422**: 938–941. (1999)

[23] Kumara W.A.S., Halvorsen B.M., Melaaen M.C., Single–Beam Gamma Densitometry Measurements of Oil–Water Flow in Horizontal and Slightly Inclined Pipes, *Int. J. Multiphase Flow*, **36**: 467–480 (2010).

[24] Da Silva M.J., Schleicher E., Hampel U., Capacitance Wire–Mesh Sensor for Fast Measurement of Phase Fraction Distributions, *Meas. Sci. Technol*., **18**: 2245–51 (2007).

[25] Shaban, H.; Tavoularis, S, The Wire–Mesh Sensor as a Two–Phase Flow Meter, *Meas. Sci. Technol.*, 26: 015306 (2015).

[26] Zhii L.S., Jin N.D., Gao Z.K., Wang Z.Y., Li D.M., The Ultrasonic Measurement of High Water Volume Fraction in Dispersed Oil–in–Water Flows, *Chem. Eng. Sci*., **94**: 271–283 (2013).

[27] Tsouris C., Norato M.A., Tavlarides L.L., A Pulse–Echo Ultrasonic Probe for Local Volume Fraction Measurements in Liquid–Liquid Dispersions, *Ind. Eng. Chem. Res*., **34**: 3154–3158 (1995).

[28] Strizzolo C., Converti J., Capacitance Sensors for Measurement of Phase Volume Fraction in Two–Phase Pipelines, *IEEE. Trans. Instrum. Meas*., **42**: 726–729 (1993).

[29] Lucas G.P., Mishra R., Measurement of Bubble Velocity Components in a Swirling Gas–Liquid Pipe Flow Using a Local Four–Sensor Conductance Probe, *Meas. Sci. Technol*., **16**: 749–758 (2005).

[30] Huang S.F., Zhang X.G., Wang D., Lin Z.H., Water Holdup Measurement in Kerosene–Water Two–Phase Flows, *Meas. Sci. Technol*., **18**: 3784–3794 (2007).

[31] Demoria M., Ferrari V., Strazza D., Poesio P., Capacitive Sensor System for the Analysis of Two–Phase Flows of Oil and Conductive Water, *Sensors. Actuat. A.*, **163**: 172–179 (2010).

[32] Strazza D., Demori M., Ferrari V., Poesio P., Capacitance Sensor for Hold–up Measurement in High–Viscous–Oil/Conductive–Water Core–Annular Flows, *Flow. Meas. Instrum*., **22**: 360–369 (2011).

[33] Sardeshpande M.V., Harinarayan S., Ranade V.V., Void Fraction Measurement Using Electrical Capacitance Tomography and High Speed Photography, *Chem. Eng. Res. Des.*, **94**: 1–11 (2015).

[34] Shang Z., Yang R., Gao X., Yang Y., An Investigation of Two–Phase Flow Instability Using Wavelet Signal Extraction Technique, *Nucl. Eng. Des.*, **232**(2): 157–163 (2004).

[35] Zhen L., Hassan Y.A., Wavelet Autocorrelation Identification of the Turbulent Flow Multi–Scales for Drag Reduction Process in Micro Bubbly Flows, *Chem. Eng. Sci.*, **61**(21): 7107–7114 (2006).

[36] Chakrabarti D.P., Das G., Das P.K., Identification of Stratified Liquid–Liquid Flow Through Horizontal Pipes by a Non–Intrusive Optical Probe, *Chem. Eng. Sci*., **62**: 1861–1876 (2007).

[37] Zong Y.B., Jin N.D., Multi–Scale Recurrence Plot Analysis of Inclined Oil–Water Two–Phase Flow Structure Based on Conductance Fluctuation Signal, *European. Phys. J. Spec. Top*., **164**: 165–177 (2008).

[38] Nguyen V.T., Euh D.J., Song C.H., An Application of the Wavelet Analysis Technique for the Objective Discrimination of Two–Phase Flow Patterns, *Int. J. Multiphase Flow*, **36**: 755–768 (2010).

[39] Tan C., Li P., Dai W., Dong F., Characterization of Oil–Water Two–Phase Pipe Flow with a Combined Conductivity/Capacitance Sensor and Wavelet Analysis, *Chem. Eng. Sci.*, **134**: 153–168 (2015).

[40] Drahos J., Zahradnik J., Puncochar M., Fialova M., Bradka F., Effect of Operating Conditions on the Characteristics of Pressure Fluctuations in a Bubble Column, *Chem. Eng. Process*., **29**: 107–115 (1991).

[41] Rosa E.S., Salgado R.M., Ohishi T., Mastelari N., Performance comparison of Artificial Neural Networks and Expert Systems Applied to Flow Pattern Identification in Vertical Ascendant Gas–Liquid Flows, *Int. J. Multiphase Flow*, **36**: 738–754 (2010).

[42] Han Y.F., Zhao A., Zhang H.X., Ren Y.Y., Liu W.X., Jin N.D., Differential Pressure Method for Measuring Water Holdup of Oil–Water Two–Phase Flow with Low Velocity and High Water–Cut, *Exp. Therm. Fluid Sci.*, **72**: 197–209 (2016).

[43] Drahos J., Cermak J., Diagnostics of Gas–Liquid Flow Patterns in Chemical–Engineering Systems, *Chem. Eng. Process*., **26**: 147–164 (1989).

[44] Park S.H., Kang Y., Kim S.D., Wavelet Transform Analysis of Pressure Fluctuation Signals in a Pressurized Bubble Column, *Chem. Eng. Sci.*, **56**: 6259–6265 (2001).

[45] Yang, T.Y., Leu, L.P., Study of Transition Velocities from Bubbling to Turbulent Fluidization by Statistic and Wavelet Multi–Resolution Analysis on Absolute Pressure Fluctuations, *Chem. Eng. Sci.*, **63**(7): 1950–1970 (2008).

[46] Matsui G., Identification of Flow Regimes in Vertical Gs Liquid Two–Phase Flows Using Differential Pressure Fluctuation, *Int. J. Multiphase Flow*, **10**: 711–720 (1984).

[47] Elperin T., Klochko M., Flow Regime Identification in a Two–Phase flow using wavelet transform, *Exp. Fluids*., **32**: 674–682 (2002).

[48] Sun Z., Shao S., Gong H., Gas–Liquid Flow Pattern Recognition Bbased on Wavelet Packet Energy Entropy of Vortex–Induced Pressure Fluctuation, *Meas. Sci. Rev.*, **13**(2), 83–88 (2013).

[49] Brauner N., Moalem Maron D., Stability Analysis of Stratified Liquid–Liquid Flow, *Int. J. Multiphase Flow*, **18**: (1992) 103–121.

[50] Marseguerra M., Minoggio S., Rossi A., Zlo E., Artificial Neural Networks Applied to Multiple Signals in Nuclear Technology, *Prog. Nucl. Energy*, **27**(4): 297–304 (1992).

[51] Cai S., Toral H., Qiu J., Archer J.S., Neural Network Based Objective Flow Regime Identification in Air–Water Two–Phase Flow, *Can. J. Chem. Eng*., **72**: 440–445 (1994).

[52] Antonopoulosdomis M., Tambouratzis T., Artificial Neural Networks for Neutron Source Localization Within Sealed Tnks, *Ann. Nucl. Energy*, **23**(18): 1477–1488 (1996).

[53] Xie T., Ghiasasiaan S.M., Karrila S., Flow Regime Identification in Gas–Liquid–Pulp Fiber Flow Based on Pressure Fluctuations Using ANN, *Ind. Eng. Chem. Res*., **42**: 7014–7024 (2003).

[54] Peng Z., Yin H., ECT and LS–SVM Based Void Fraction Measurement of Oil–Gas Two–Phase Flow, *Iran. J. Chem. Chem. Eng. (IJCCE)*, **29**(1): 41–50 (2010).

[55] Salgado C.M., Pereira C.M.N.A., Schirru R., Brandão L.E.B., Flow Regime Identification and Volume Fraction Prediction in Multiphase Flows by Means of Gamma–Ray Attenuation and Artificial Neural Networks, *Prog. Nucl. Energy*, **52**: 555–562 (2010).

[56] Zhang C., Zhang T., Yuan C., Oil holdup Prediction of Oil–Water Two Phase Flow Using Thermal Method Based on Multiwavelet Transform and Least Squares Support Vector Machine, *Expert Syst. Appl.*, **38**: 1602–1610 (2011).

[57] Bin S., Hong W., Identification Method of Gas–Liquid Two–Phase Flow Regime Based on Wavelet Packet Energy Feature and PNN, International Conference on ICCE2011, *AISC*, **112**: 595–603 (2011).

[58] Nazemi E., Feghhi S.A.H., Roshani G.H., Gholipour Peyvandi R., Setayeshi S., Precise Void Fraction Measurement in Two–Phase Flows Independent of the Flow Regime Using Gamma–Ray Attenuation, *Nucl. Eng. Technol.*, **48**: 64–71 (2015).

[59] Cong T., Su G., Qiu S., Tian W., Applications of ANNs in Flow and Heat Transfer Problems in Nuclear Engineering: A Review Work, *Prog. Nucl. Energy*, **62**: 54–71(2013).

[60] Daubechies I., The Wavelet Transform, time–Frequency Localization and Signal Analysis, *IEEE. T. Inform. Theory*, **36**: 961–1005 (1990).

[61] Daubechies I., "Ten lectures on Wavelets. Society for Industrial and Applied Mathematics", SIAM Publication. Philadelphia. (1992).

[62] Jana K., Das G., Das P.K., The hydrodynamics of Liquid–Liquid Upflow Through a Venturimeter, *Int. J. Multiphase Flow*, **34**: 1119–1129 (2008).

[63] Jafari, M.R., Salahshoor K., Adaptive Predictive Controllers Using a Growing and Pruning RBF Neural Network, *Iran. J. Chem. Chem. Eng. (IJCCE)*, **30**(2): 125–138 (2011).

[64] Azari A, Shariaty–Niassar M, Short–Term and Medium–Term Gas Demand Load Forecasting by Neural Networks, *Iran. J. Chem. Chem. Eng. (IJCCE)*, **31**(4): 77–84 (2012).

[65] Karimi H., Yousefi F., Rahimi M.R., Correlation of Viscosity in Nanofluids Using Geneticalgorithm–Neural Network (GA–NN), *Heat. Mass. Transfer. J.*, **11**: 1417–1425 (2011).

[66] Timung S., Mandal T.K., Prediction of Flow Pattern of Gas–Liquid Flow Through Circular Microchannel Using Probabilistic Neural Network, *App. Soft. Comput.*, **13**: 1674–1685 (2013).

[67] Specht D. F., Probabilistic Neural Networks, *Neural Networks*, **3**: 109–118 (1990).

[68] Sayyad H., Manshad A.K., Rostami H., Application of Hybrid Neural Particle Swarm Optimization Algorithm for Prediction of MMP, *Fuel*, **116**: 625–633 (2014).

[69] Bulsari A.B., "Neural Networks for Chemical Engineers", Amsterdam, Elsevier, (1996).

[70] Azizi S., Ahmadloo E., Awad M.M., Prediction of Void Fraction for Gas–Liquid flow in Horizontal, Upward and Downward Inclined Pipes Using Artificial Neural Network, *Int. J. Multiphase Flow*, **87**: 35–44 (2016).

[71] Terrence L.F., "Feedforward Neural Network Methodology", New York, Springer, (1999).